

Advanced translational cosmetics: using the world's first non-invasive Bioimpedance 3D Bioprinted skin chips to link cosmetics lab testing to humans.

McGuckin, Colin^{1*}; Bechettoille, Nicolas²; Legues¹, Maxime; Milet, Clement¹; Besseyre, Raphael¹; Boyer, Maxime¹; Ferrier, Wendy¹; Sanchez, Alexia²; Forraz, Nico¹; Vogelgesang, Boris².

¹ CTIBIOTECH, Lyon, France; ² Gattefosse SAS, Saint-Priest Cedex, France

* Colin McGuckin, CTIBIOTECH, Bat A16, 5 Avenue Lionel Terray, Meyzieu-LYON, France. +33967107455. c.mcguckin@ctibiotech.com

Abstract

Introduction: *In vivo* cosmetics donor testing remains the most expensive stage to creating advanced safe cosmetics. Solutions to making safer cosmetics requires better testing which is why we have developed the world's first 3D Bioprinted oily skin model which can measure the same non-invasive electrical activity as on humans, while at the same time giving normal laboratory read-outs. Bioimpedance, which has long been used for general body composition testing can also be applied at the surface skin level, to evaluate changes in the local skin environment. Here we aimed to combine laboratory and *in vivo* parameters for better cosmetics testing.

Methods: Keratinocytes, fibroblasts and sebocytes were isolated from donations of human skin sample following elective surgery and ethical consent. Cells were mixed with a bioink and cartridge into a CELLINK 3D bioprinter. 3D models were printed and bioimpedance readings were made and treatments with known modulators of oil production. Changes in cellular viability were assessed with Live/Dead staining and Alamar Blue and oil production was further evaluated by the standards Oil Red O and Nile Red.

Results: Significant differences were observed using the bioimpedance device. These variations were correlated with viability assays and oil production assays in response to the lipid modulators, Linoleic Acid and TOFA. Our 3D model was validated for oil secretion screening and new bioimpedance probes were designed and validated for both supernatant and 3D models.

Conclusion: Non-invasive and fast analysis of bioimpedance can be performed on 3D models and linked to *in vivo* data.

Keywords: 3D Bioprinting; tissue engineering, bioimpedance, translational, lipids.

1. Introduction.

Bioimpedance or bioelectrical impedance analysis (BIA) has been developed for some decades now [1]. It is a very useful parameter because of several advantages: it is inexpensive, very easy to use, and it is a non-invasive technique. Bioimpedance is the ability of a biological tissue to oppose an applied electric current flow. The result a quantifiable value expressed in Ohm (Ω).

Over the past two decades, bioimpedance has been used in a variety of applications, such as *in vivo* blood characterization [2], fish flesh quality assessment [3], myocardial ischemia detection [4], biological barrier monitoring [5], global monitoring of biological tissue composition [6] and, last but not least, human body composition [7, 8]. It is now possible to monitor diet and health directly from home using bioimpedance weigh scales. Small devices also arrived on the market to evaluate for example percentage of moisturization of our skin (“Digital Moisture Monitor”).

Sebum is one of the keys to maintain skin homeostasis. It has many properties contributing to regulating skin microbiome, antioxidants properties and anti-aging characteristics [9]. Sebum is a complex mélange of triglycerides, wax esters, squalene and free fatty acids, amongst other components still being identified in both normal and dysregulated skin [10, 11].

Different sebaceous models already exist, including cell lines like SZ95 [12], and most recently a new *ex vivo* model of human sebaceous glands isolated from human skin donor sample [13]. 3D Bioprinting also produced an interesting model of microsebaceous gland 3D bioprinted for oil secretion screening [14]. These current models are interesting, but lack the fast and non-invasive validation of active ingredients.

Therefore, we have combined 3D bioprinted technology to produce relevant models, with bioimpedance to produce rapid *laboratory* data that eventually can be linked with *in vivo* results.

2. Materials and Methods.

2.1. Sample collection

Sebocytes, fibroblasts and keratinocytes were isolated from donated human skin samples after informed consent. Sample collection was performed in accordance with French and European ethical guidelines and regulations applicable in local hospitals in Lyon, France. Optimal transport conditions were used to ensure the best viability of the samples.

2.2. Cells isolation and amplification

Fibroblasts and Keratinocytes were isolated from human skin donors using enzymatic dissociation and grown in 6-well plates (Corning®) using RPMI 1640 medium (HyClone™, GE Healthcare) supplemented with 15% FBS (HyClone™), cyprofloxacin (4 µg/mL) and EpiLife® medium (Gibco™, ThermoFischer) supplemented with Human Keratinocytes Growth Supplement (HKGS, Gibco™) respectively.

Sebocytes were isolated from mechanically extracted sebaceous glands as described in our previous studies and grown in Seb4Gln medium with fibronectin coating (1.3 µg/cm²) [13]. During the entire isolation process, viability of cells was tested using a LUNA-FL™ Dual Fluorescence Cell Counter (Logos Biosystems, France).

2.3. Bioinks preparation

After amplification in 225 cm² flasks, cells were harvested with Tryple enzyme (Tryple Select 1X, Gibco™), centrifuge and count using a LUNA-FL™ Dual Fluorescence Cell Counter (Logos Biosystems, France).

Sebocytes and fibroblasts were mixed together with a specific bioink allowing the cells to grow and spread (Cellink, Goteborg, Sweden) to create the dermis layer. Keratinocytes were mixed separately with a second bioink (Cellink) to create the epidermis layer. Bioinks containing cells were then placed into 3 ml cartridges (Optimum® EFD, Nordson, USA).

2.4. 3D Bioprinting

Computer aided design software, Sketchup (Trimble, USA) was used to create separate 3D models for dermis part and epidermis part. 3D models were then assembled in a slicing software, SLIC3R, to create a G-code file, suitable for complex 3D bioprinting. The G-code

was then transferred to a USB stick and connected to a Bio X™ 3D bioprinter (Cellink). The 3D bioprinting process was performed under sterile conditions, under a laminar flow hood to avoid contamination.

The cartridges containing the bioinks were placed in the defined print heads, the G-code selected and the models 3D bioprinted in 12-well plates according to CTIBiotech's optimization protocols.

2.5. Maturation in culture

After 3D Bioprinting, models were first crosslinked with Calcium Chloride (Crosslinking agent, Cellink) for 5 minutes, following supplier protocol and rinsed one time with PBS 1X (Corning®).

3D printed models were grown for 14 or 21 days in Transwell® culture inserts (VWR, USA), including the stages of dermal maturation, epidermal differentiation, air-liquid interface and cornification of the bioprinted models.

2.6. Treatments of models

In order to modulate lipid production, 3D models of sebaceous micro-glands were treated in triplicates for 5 days: Linoleic acid (Sigma-Aldrich, St Quentin Fallavier, France), and TOFA (5-(tetradecyloxy)-2-furoic acid, Sigma-Aldrich) as controls and 3 test active ingredients A1, A2 and A3 (Gattefosse, Lyon, France). Properties of the actives were not known at the time of the experiment and were blind tested.

2.7. Viability analysis

3D models were analyzed every 7 days to evaluate viability and morphology inside the bioink. Live/Dead™ kit reagents (Invitrogen, USA) was used for viability analysis. Calcein AM (live cells) and Ethidium homodimer-1 (dead cells) for 30 minutes before microscopic analysis. Live cells were analyzed at 494/517 nm and dead cells at 528/617 nm (excitation/emission) on a Nikon Ti-S Eclipse fluorescence microscope (NIKON, Japan).

2.8. Viability quantification

AlamarBlue™ Cell Viability reagent (Invitrogen) was directly added in each individual 3D models well and incubated for 4 hours. Supernatants were collected and transferred to a black-walled 96-well plate. Fluorescence was quantified on a microplate reader (Tecan Spark®) at 550 nm, excitation and 590 nm, emission.

2.9. Oil production analysis

After fixation with formaldehyde 4% w/v (Sigma-Aldrich), 3D models were stained with 1 µM Nile Red (Sigma-Aldrich) and 1 µg/ml 4',6-diamidino-2-phenylindole (DAPI, Sigma-Aldrich). Variation in lipid production was quantified after treatments. After fixation and rinsing of the 3D models, a filtered solution of Oil Red O was added to the models. 3D models were rinsed again and Oil Red O-stained lipids were eluted using 100% isopropanol. Quantity of lipids was finally measured with a spectrophotometer (TECAN Spark®, Switzerland) at 510 nm.

2.10. Bioimpedance measurement

After 5 days of treatment, supernatants were collected, sampled and measured on an Electric Bridge Resistance Impedance Capacitance Inductance Digital LCR Meter (East Tester®, China) calibrated in the 10 kHz range.

2.11. Histology

At the end of the experiment, 3D models were rinsed once with PBS 1X (Corning) and fixed in formaldehyde 4% w/v (Sigma-Aldrich), before dehydration in alcohol crescent baths and clarification in xylene. Samples were then embedded in paraffin and sectioned into 5 µm thick slices. Hematoxylin, eosin and saffron coloration was performed on the slide after a rehydration process.

3. Results.

3.1. Production of 3D Bioprinted models for lipid screening

As 3D bioprinting is an additive manufacturing technology, the first step was to design 3D models to mimic basic skin to evaluate lipid production. Our first model was a dermis based structure with mixed layers of sebocytes and fibroblasts only. The second model was a dermis and epidermis model with a layer of bioink containing keratinocytes on top of the dermis model (**Figure 1A**). 3D Models were produced on Bio X 3D Bioprinter from Cellink and reproducible models were obtained (**Figure 1 B,C**).

3D models were grown in Transwell® culture insert as described previously (first described at IFSCC2020, Yokohama, Henry Maso award 2022) for 3 weeks after bioprinting for dermis models, and 47 days after bioprinting for models with dermis and epidermis.

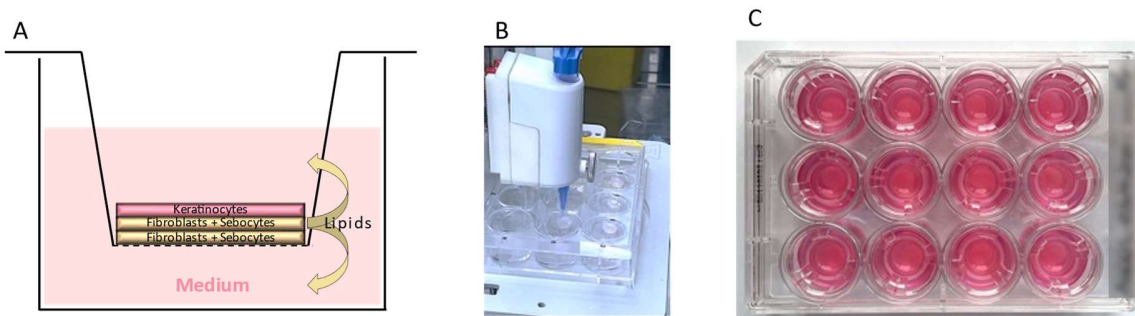


Figure 1: Design and creation of 3D models using 3D Bioprinting technology; A) design of model, B) 3D Bioprinting of models in a 12-well plate, C) 3D models in Transwell® Culture inserts.

Viability of both models was assessed using Live/Dead reagents and fluorescence microscopical analysis. We observe an overall very good viability of the cells inside the bioink for both types of models (**Figure 2**) with very few dead cells 7 and 14 days after bioprinting demonstrating the relevance of the selected bioinks. We can also confirm the 3D morphology of cells in the bioinks.

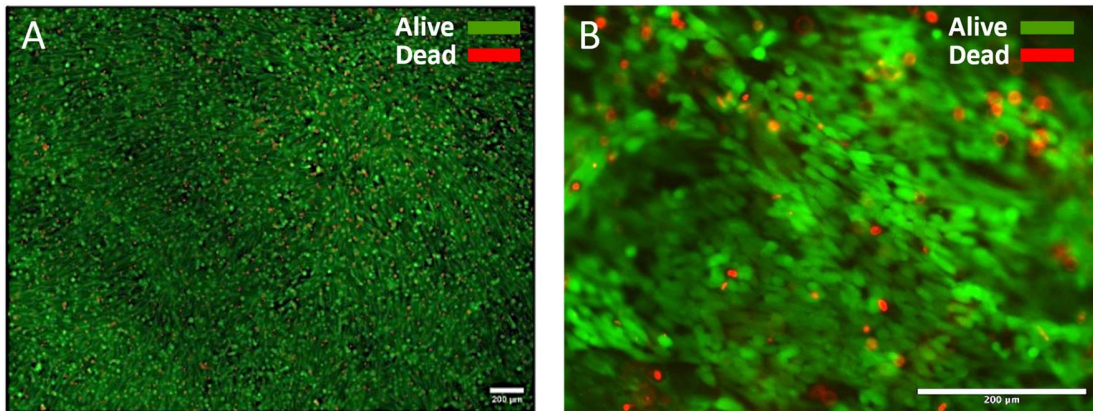


Figure 2: Viability analysis of 3D Bioprinted models after Live/DeadTM staining and fluorescence microscopy analysis, A) after 7 days of maturation; B) after 14 days of maturation.

At the end of maturation, models were analysed by histology after paraffin embedding and HES coloration. For the dermis model, 21 days after bioprinting, results showed rounded structures similar to an *in vivo* sebaceous gland (**Figure 3A**). For the dermis and epidermis model, 47 days after bioprinting, results showed multilayered, differentiated and cornified epidermis developed on the dermis. The dermal-epidermal junction (DEJ) was defined, separated, organised and differentiated (**Figure 3B**).

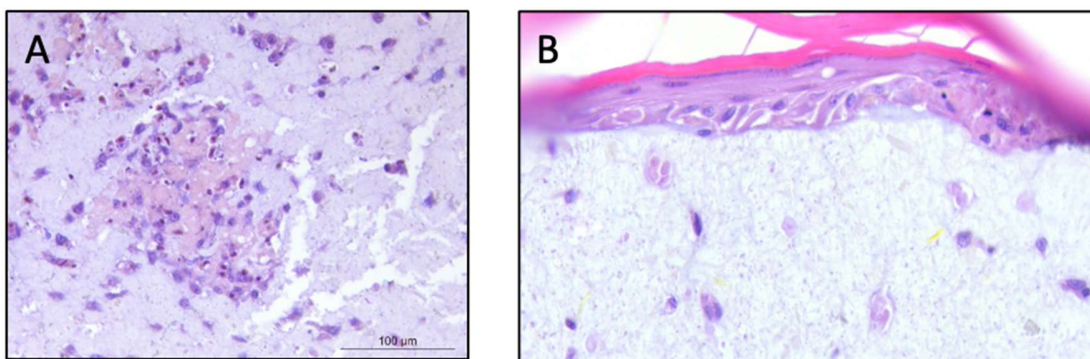


Figure 3: Microscopic analysis of Hematoxylin, Eosin and Saffron coloration (HES), A) 21 days after 3D Bioprinting for dermis 3D model (fibroblasts and sebocytes only), B) 47 days after 3D Bioprinting for dermis and epidermis models (Fibroblasts, sebocytes and keratinocytes 3D Bioprinted).

Interestingly, the keratinocytes survived the 3D bioprinting process and were able to create a cornified epidermis even mixed with the bioink. Maturation and differentiation time were, however, noticeably longer than the dermis model with fibroblasts and sebocytes only.

3.2. Evaluation of metabolic activity

As our aim was to develop a model for lipid screening, we first validated this model with well-known lipid modulators. Linoleic acid, as a lipid stimulator, and TOFA as an inhibitor of lipid accumulation. We also assessed treatment of 3 cosmetic active ingredients, A1, A2 and A3 in single blind test.

First, we checked viability after treatments using the Alamar Blue test. Results showed a basal level of metabolic activity for the untreated control (**We then** observed a very slight increase in viability for linoleic acid and a significant reduction for TOFA, expressing a potential toxicity of TOFA under these conditions.

Finally, active ingredient A2 showed a slight increase in viability, similar to that of linoleic acid, while active ingredients A1 and A3 showed a slight but less significant reduction than with the TOFA treatment.

Figure 4). We then observed a very slight increase in viability for linoleic acid and a significant reduction for TOFA, expressing a potential toxicity of TOFA under these conditions.

Finally, active ingredient A2 showed a slight increase in viability, similar to that of linoleic acid, while active ingredients A1 and A3 showed a slight but less significant reduction than with the TOFA treatment.

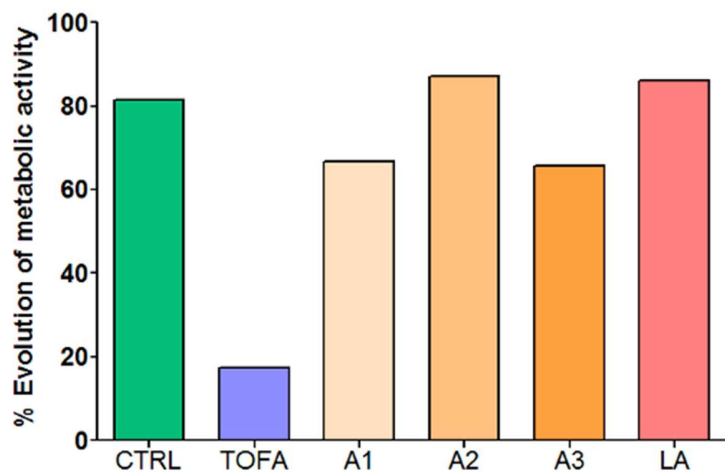


Figure 4: Analysis of viability of 3D models after treatment with known lipid modulators (TOFA (50 µM) and Linoleic acid 1mM (LA)) and actives A1, A2 and A3.

3.3. Evaluation of lipid production

In order to assess the lipid production, Nile Red staining was carried out on the 3D models after treatments with lipid modulators (**Figure 5**). Fluorescence microscopic analysis revealed a significant increase of lipid droplet after treatment with Linoleic acid, as expected, compared to the untreated condition. We observed, more lipid droplets as well as bigger lipid droplets inside the structures.

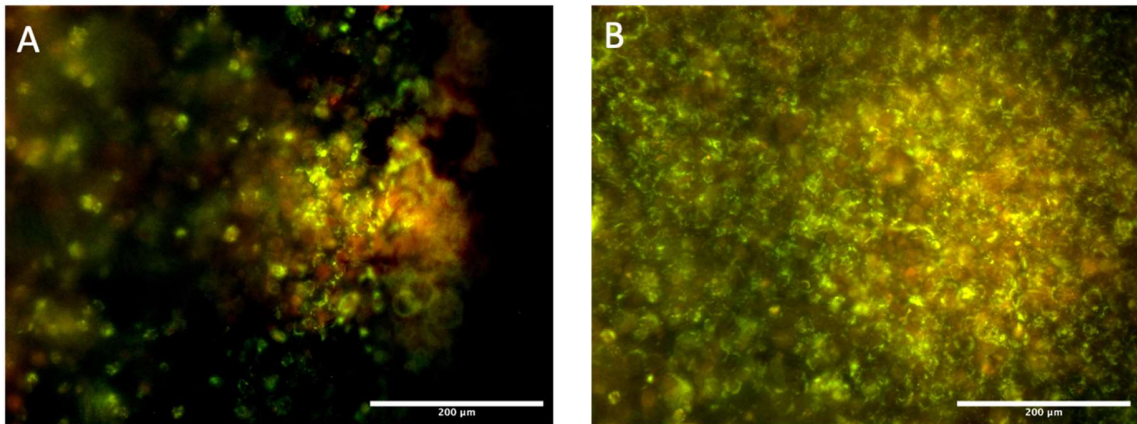


Figure 5: Fluorescence microscopic analysis of 3D Bioprinted models (fibroblasts and sebocytes) after Nile Red staining; A) Untreated control medium only, B) Linoleic acid 1 mM.

To confirm Nile Red results, Oil Red O staining was performed (**Figure 6**). Microscopic observations of the 3D models validated the level of lipids in the different conditions.

First, a slight reduction was observed in TOFA condition compared to the untreated control. On the opposite, a substantial increase was detected in Linoleic acid condition. Similarly to the Nile Red observations, Linoleic acid condition showed sebocytes rich in lipids (**Figure 6C**).

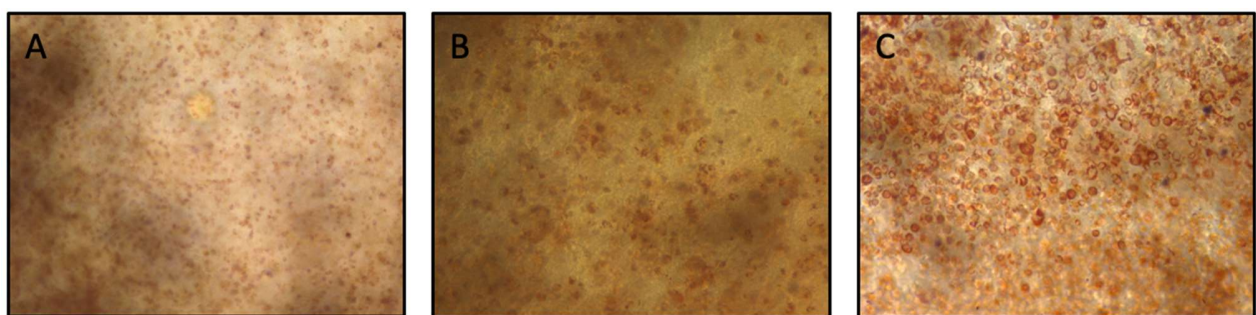


Figure 6: Microscopic analysis of 3D Bioprinted models (fibroblasts and sebocytes) after Oil Red O staining; A) Untreated control medium only, B) TOFA 50 μ M, C) Linoleic acid 1 mM.

3.4. Bioimpedance

3.4.1. Probe design

Prior to the measurement of bioimpedance on 3D models and supernatant, adaptation of the probes needed to be performed. Indeed, the probes supplied with the device were not suitable for 3D models measurement.

We decided to develop 2 probes, first one is specific for 3D models, on which we can place the 3D model and avoid any operator variability. (**Figure 7A**). The second probe was designed to measure the supernatant, using a small container into which the supernatant can be added. (**Figure 7B**).

These probes were ingeniously designed to enhance operator handling and were compatible with the supplier's probes to be connected to.

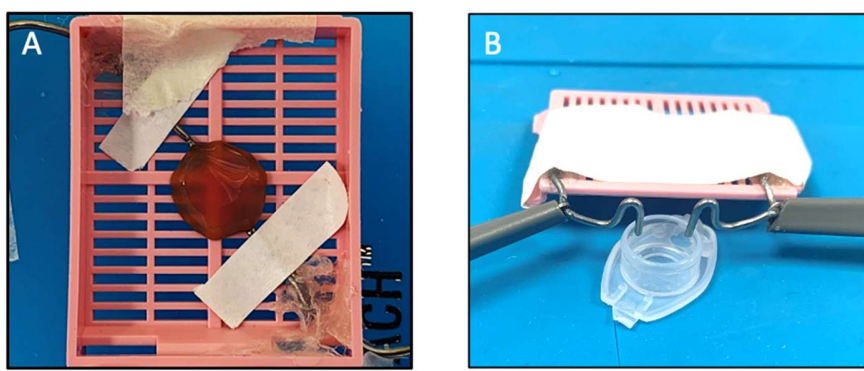


Figure 7: Design of probes for Bioimpedance analysis of 3D Bioprinted models and supernatant.

3.4.2. Validation of bioimpedance device

To demonstrate the capability of bioimpedance to detect changes in lipid production, we collected supernatant at days 0, 1, 2 and 5 after treatment with lipid modulator, and performed bioimpedance readings using the second probe (**Figure 8**).

Interestingly, for all conditions, the bioimpedance level increased over time from day 0 to day 2, which was expected as lipids tend to accumulate in sebocytes. Day 5 finally showed significant differences between conditions.

TOFA treatment, slightly reduced bioimpedance level compared to the untreated control, certainly reflecting the inhibition of lipid accumulation. In contrast, Linoleic Acid, and actives A1, A2 and A3 showed significant decrease of the bioimpedance signal, probably expressing the release of lipids in the supernatant between day 2 and day 5.

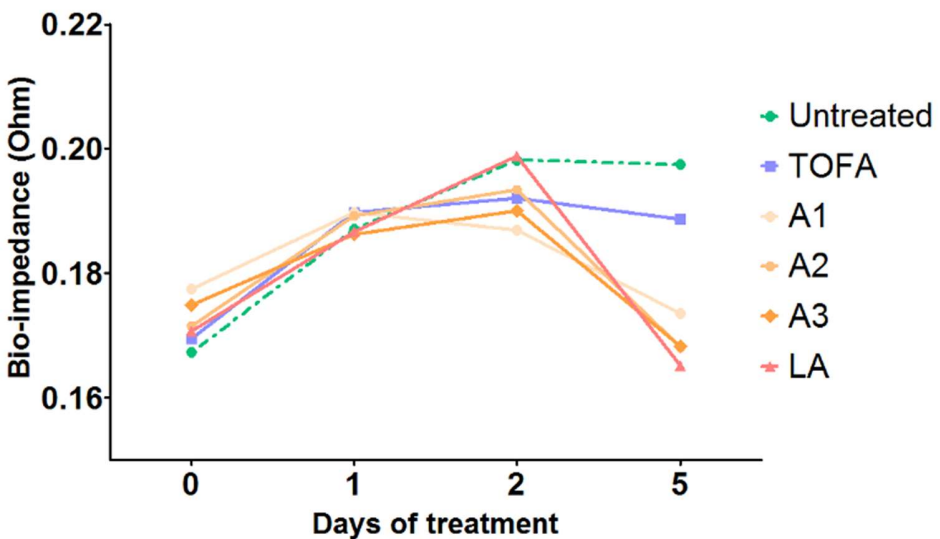


Figure 8: Evolution of Bioimpedance reading on supernatant after treatment with lipid modulators: TOFA 50 μ M, Linoleic Acid 1 mM and actives A1, A2 and A3.

At the end of the experiment, 3D models were collected at day 5 for bioimpedance analysis. After TOFA treatment, we observed a decrease of bioimpedance signal compared to untreated control (Figure 9). This correlate with Oil Red O, Nile Red and supernatant bioimpedance results.

On the other hand, Linoleic acid and actives A1 and A2 revealed an interesting trend as bioimpedance levels slightly increased compared to untreated control. This can be explained by the fact that lipids were already released in the supernatant.

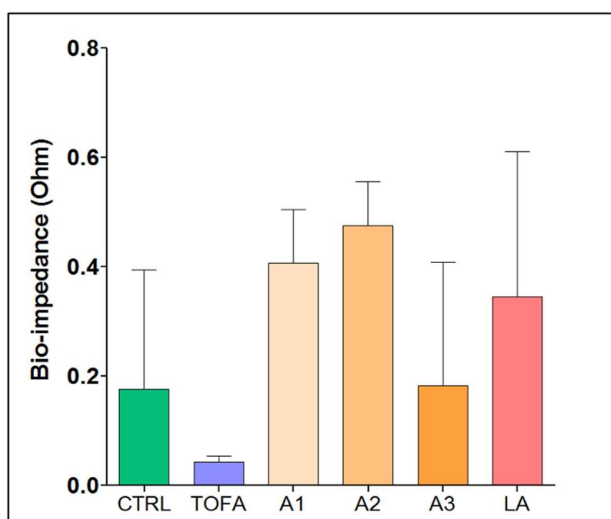


Figure 9: Bioimpedance analysis of 3D models after 5 days of treatment with Lipids modulators: TOFA 50 μ M, Linoleic Acid 1 mM and actives A1, A2 and A3.

The sebocytes accumulate lipids and eventually release their contents by holocrine secretion as the cells disintegrate. Therefore, as lipids were released, less sebocytes are present in 3D models explaining the reduction of bioimpedance levels.

4. Discussion.

In recent years, bioimpedance has been widely used to monitor our personal health and especially our body composition with the advent of connected scales. Such non-invasive instruments are important for athletes but also for anyone and everyone to monitor their health and adjust their diet and lifestyles accordingly. Here in this study, we have evaluated the use of bioimpedance for screening of active ingredient on our 3D bioprinted skin models and specially for lipid production.

The disruption of sebum production can indeed contribute to the development of oily or dry skin and can lead to common skin diseases, including acne or atopic dermatitis [11]. We have shown it was possible to use 3D bioprinting to create a relevant *in vitro* full skin model including sebaceous glands [14]. We have also shown that it was possible to modulate models to contain a variety of cell types including macrophages [15]. Here, we have therefore enhanced our model by improving *in vitro* lipid production and validated the use of a rapid non-invasive technology, bioimpedance, for the detection of lipid secretion.

Differences in bioimpedance were seen compared to untreated models. Treated models containing sebocytes had reproducible oil production which was increased by Linoleic acid and reduced by TOFA and remarkably this was characterized by significant changes in bioimpedance in both the printed models and the supernatant. The bioimpedance measurements were correlated with viability, and lipid production results. This demonstrated the accuracy of the technique to non-invasively measure differences in skin oil activity.

Rapid development and validation of effective dermo-cosmetic products requires the development of innovative preclinical models and the use of state-of-the-art technologies.

By combining our 3D Bioprinting skin model with bioimpedance, we aim to take a major step forward towards better and more effective cosmetic products and to help the cosmetics industry accelerate towards final donor testing more effectively.

5. Conclusion.

Non-invasive methods to understand live donor testing have been seriously discussed for many years for ethical reasons. However, linking such data to the laboratory to make the development chain of cosmetics more effective has not been easy. Bioimpedance, linked to oil production data provides an important step forward to help create effective and safe cosmetics, since the full-thickness models described here and linked with a simple chip system, accurately detect changes within the skin model. Therefore, our models allow advanced translational lab-to-donor data to help bring sophisticated cosmetics ingredients to market faster, safely and more affordably.

Acknowledgments.

We would like to deeply thanks Natecia hospitals, Lyon, Clinique Saint-Vincent de Paul, Bourgoin-Jallieu, the doctors, nurses and donors of skin tissues for making possible the collection of skin and therefore the production of skin cells.

We thank as well “La Région Auvergne-Rhône Alpes” and BPI France for supporting our 3D Bioprinting platform. We are also thankful to Mr Mathieu Lacroix and Ms Tiffany Luangvannasy for operation of the biobanking and skin facilities.

Conflict of Interest Statement.

NONE.

References.

1. Creason S.C., Loyd R. J., and Smith D. E., (1972), Evaluation of a computerized sampling technique for digital data acquisition of high-speed transient waveforms. Application to cyclic voltammetry. *Analytical Chemistry* 1972 44 (7), 1159-1166.
2. Dai T, Adler A. (2009), In Vivo Blood Characterization From Bioimpedance Spectroscopy of Blood Pooling. *IEEE Transaction on Instrumentation and Measurement*, Vol. 58, N°. 11, pp. 3831-3838.

3. Duncan M, Craig S.R., Lunger A. N., Kuhn D. D., Salze G, McLean E, Bioimpedance assessment of body composition in cobia *Rachycentron canadum* (L. 1766), *Aquaculture*, (2007), Volume 271, Issues 1–4, Pages 432-438.
4. Yufera A, Rueda A, Member, IEEE, Muñoz JM, Doldán R, Leger G, and Rodríguez-Villegas EO, (2005), A Tissue Impedance Measurement Chip for Myocardial Ischemia Detection. *IEEE Transaction on Circuits and Systems I: Regular Papers*, Vol. 52, Nº. 12.
5. Cacopardo L, Costa J, Guazzelli N, Giusti S, Meucci S, Corti A, Mattei G, Ahluwalia A, (2019), Real-time cellular impedance monitoring and imaging in a dual-flow bioreactor. *Biomedical Science and Engineering*, volume 3(s3):104.
6. Lamlih A. Design of an Integrated Bioimpedance Measurement System for Chronic Monitoring of Biological Tissue Composition, (2018), *Optics / Photonic. Université Montpellier, English*. NNT : 2018MONT070.
7. Lee SY, Gallagher D, (2008), Assessment methods in human body composition. *Current Opinion in Clinical Nutrition and Metabolic Care: September 2008 - Volume 11 - Issue 5 - p 566-572.*
8. Lukaski, H C, (1987), Methods for the assessment of human body composition: traditional and new. *The American Journal of Clinical Nutrition*. Volume 46, Issue 4, October 1987, Pages 537–556.
9. Smith K. R., Thiboutot D. M. (2008). Thematic review series: skin lipids. Sebaceous gland lipids: friend or foe?. *Journal of Lipid Research*, 49(2), 271–281.
10. Zouboulis, C. C., Picardo, M., Ju, Q., Kurokawa, I., Törőcsik, D., Bíró, T., & Schneider, M. R. (2016). Beyond acne: Current aspects of sebaceous gland biology and function. *Reviews in Endocrine & Metabolic Disorders*, 17(3), 319–334.
11. Shi V. Y, Leo M, Hassoun L, Chahal D. S, Maibach H. I, Sivamani, R. K. (2015). Role of sebaceous glands in inflammatory dermatoses. *Journal of the American Academy of Dermatology*, 73(5), 856–863.
12. Zouboulis CC, Seltmann H, Neitzel H, Orfanos CE. (1999), Establishment and characterization of an immortalized human sebaceous gland cell line (SZ95). *J Invest Dermatol*. 1999 Dec;113(6):1011-20.

13. de Bengy A. F, Forraz N, Danoux L, Berthelemy N, Cadau S, Degoul O, Andre V, Pain S, McGuckin C, (2019). Development of new 3D human ex vivo models to study sebaceous gland lipid metabolism and modulations. *Cell Proliferation*, 52(1), e12524.
14. Milet C, Simmering A, Legues M, Ferrier W, Forraz N, Bussmann T, Seidel J, Reuter J H, McGuckin C, (2020), Creation of a 3D printed sebaceous gland model for oil secretion screening and burns research. *IFSCC Congress 2022 Yokohama*.
15. Legues, M., Milet, C., Forraz, N., Berthelemy, N., Pain, S., Andre, V., Cadau, S., & McGuckin, C. (2020). The world's first 3D Bioprinted immune skin model for screening drugs and ingredients for normal and inflamed skin. *IFSCC 2020 Yokohama*.